Imaging properties of a tetra wedge readout*

Liu Yong-An(刘永安)[a)†], Yan Qiu-Rong(鄢秋荣)[a)], Sai Xiao-Feng(赛小锋)[a)], Wei Yong-Lin(韦永林)[a)], Sheng Li-Zhi(盛立志)[a)], Yang Hao(杨 颢)[a)b)], Hu Hui-Jun(胡慧君)[a)b)], and Zhao Bao-Sheng(赵宝升)[a)]

[a)] *State Key Laboratory of Transient Optics and Photonics, Xi'an Institute of Optics and Precision Mechanics, Chinese Academy of Sciences, Xi'an* 710119, *China*

[b)] *Graduate University, Chinese Academy of Sciences, Beijing* 100049, *China*

(Received 10 November 2010; revised manuscript received 2 December 2010)

The decoding principle of a tetra wedge anode, which is a development of the wedge and strip anode, is described. The influence of charge cloud size on decoding accuracy is studied using the Monte Carlo method. Simulation results show that the decoding error is large when the size of charge clouds collected by the anode is small. Thus, the charge clouds collected by the tetra wedge anode should reach a necessary size to ensure accurate decoding. Finally, using the ultraviolet photon counting imaging system, the linearity and the spatial resolution of the system are tested. Experimental results show that the system has a good linearity and the spatial resolution is better than 100 μm.

Keywords: detectors, photon counting imaging, tetra wedge anode, microchannel plate

PACS: 85.60.Bt, 85.45.Bz, 29.40.Gx **DOI:** 10.1088/1674-1056/20/6/068503

1. Introduction

Photon-counting imaging detectors, based on a microchannel plate (MCP) and a position-sensitive anode, can reconstruct the image of a target in a period of time using the position-sensitive photon-counting technique. These detectors are very useful devices when the light source is weak and a large dynamical range is needed, and they have been widely used for observing space in astronomy, detecting nuclear radiation and measuring ultraweak luminescence and spectra in biology.[1−4] There are a variety of position-sensitive anodes that can be used as the decoder for a photon-counting imaging detector, such as resistive anodes,[5] wedge and strip anodes (WSA),[6] vernier anodes[7] and delay-lines.[8] The WSA typifies the family of conductive charge division readouts using the geometrical charge division technique. Such devices have several advantages, such as a simplified anode design and reduced manufacture process requirements, requiring only a small number of charge measurement channels, and enhanced resolution. Although the traditional three-electrode WSA has advantages in its simple production, resolution and linearity performance, in practice, the electrode theoretical dynamic range is only 0 to 0.5, which limits the performance of spatial resolution to some extent. Here, a tetra wedge anode (TWA),[9] with the electrode theoretical dynamic range extended from 0 to 1, is designed to optimize the conventional three-electrode WSA and improve the spatial resolution of the anode.

In this study, the decoding principle of the TWA is briefly introduced. Monte Carlo simulations are presented and the influence of charge cloud size on decoding accuracy is studied. Finally, the imaging performance of the TWA collector is tested using a ultraviolet photon-counting imaging system based on the induction readout.[10−13]

2. Photon counting imaging system and tetra wedge anode

Figure 1(a) shows the sketch of the photon-counting imaging system based on the induction readout. The system consists of an UV source, attenuator and filter, MCPs, Ge layer and its substrate, position-sensitive anode, amplifier and a data acquisition and processing system. The MCPs, Ge layer and its substrate and position-sensitive anode are in the vacuum chamber, but the MCPs and Ge layer with its substrate can also be sealed in an intensifier tube. In this system, the electrons ejected from the MCP are incident on the Ge layer. The resistance of the Ge layer should be chosen such that the time constant

*Project supported by the National Natural Science Foundation of China (Grant Nos. 31070887 and 10878005).

†Corresponding author. E-mail: liuan86@126.com

© 2011 Chinese Physical Society and IOP Publishing Ltd

for event-charge dissipation is significantly longer than that of the charge-measurement process. Therefore, the charge can be positioned long enough for the external position-sensitive anode to determine its centroid position. The detailed structure and operating principles of the UV photon-counting imaging system based on Ge-induction readout have been introduced elsewhere.[10−13]

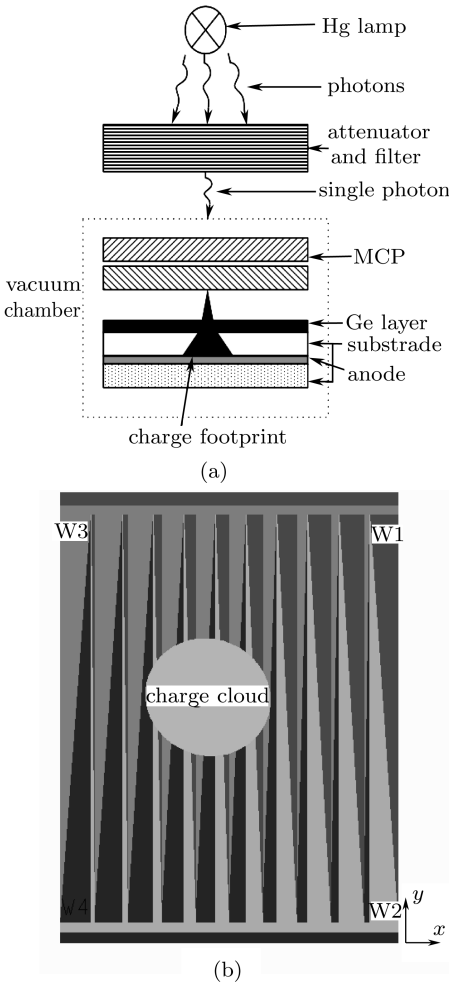


Fig. 1. Sketch of photon-counting imaging system based on an induction readout (a), and principle sketch of the position-sensitive tetra wedge anode (b).

Figure 1(b) shows the planar structure sketch of the TWA collector. The TWA is a planar structure device composed of four electrodes, which can be organized as two pairs of interlocking comb-like electrodes. Each electrode occurs only once in each pattern pitch and the typical pitch is 1 mm–2 mm. This novel geometry allows the theoretical dynamic range of the pairs of electrodes used to encode each axis to vary from 0 to 1. In practice, because of manufacturing limitations and interelectrode capacitance considerations, the theoretical dynamic range can be reduced by ∼1/3. However, this still leaves the TWA with a factor 2 advantage in imaging performance over the traditional WSA. This advantage can be utilized either to increase spatial resolution, or to reduce the pulse processing time for a given signal-to-noise ratio and hence increase the maximum event rate for a given spatial resolution.[14] The resulting event coordinates can be given by

$$X = \frac{Q_{\mathrm{W1}} + Q_{\mathrm{W2}}}{Q_{\mathrm{W1}} + Q_{\mathrm{W2}} + Q_{\mathrm{W3}} + Q_{\mathrm{W4}}},$$
$$Y = \frac{Q_{\mathrm{W1}} + Q_{\mathrm{W3}}}{Q_{\mathrm{W1}} + Q_{\mathrm{W2}} + Q_{\mathrm{W3}} + Q_{\mathrm{W4}}}, \qquad (1)$$

where Q_{W1}, Q_{W2}, Q_{W3} and Q_{W4} are the charge signals collected by the W1, W2, W3 and W4 electrodes for each event, respectively.

3. Monte Carlo simulation

3.1. Influence of charge cloud size on decoding accuracy

A relevant study[15] suggests that the MCP radial charge distribution is quasi-Gaussian. The charge clouds collected by the charge division anodes should reach a certain size to ensure accurate decoding and good linearity. Smith *et al.*[16] has simulated the modulation of WSA and in this paper we adopt a similar Monte Carlo approach to investigate the influence of charge cloud size on the decoding accuracy of the TWA collector. To simplify the model, we use an ideal anode (insulation gap width of 0), which is a rectangular TWA as shown in Fig. 1(b), and the TWA pattern has a pitch of 1.5 mm and collection area of 45 mm × 45 mm.

$$N(r) = \begin{cases} \left(\dfrac{1}{\sigma\sqrt{2\pi}}\,\mathrm{e}^{-r^2/(2\sigma^2)}\right) - \left(\dfrac{1}{\sigma\sqrt{2\pi}}\,\mathrm{e}^{-1/(2\times 2.75^2)}\right), & r \le 2.75\sigma, \\ 0, & r > 2.75\sigma. \end{cases} \qquad (2)$$

Expression (2) gives the function of Gaussian distribution used in the simulation, where the small negative constant term gives the distribution a root at 2.75σ, and for radii larger than 2.75σ the distribution is set to be zero to avoid the infinite tail of a true Gaussian. The simulation method is as follows:

(i) Given the centroid position of an event, to generate a series of different sizes of charge clouds which have the same centroid position as the event. Each electric charge cloud contains N electrons and the electron distribution function is Gaussian distribution function.

(ii) To judge the location of each electron and the total number of electrons on each electrode. On the assumption that each electron represents a unit electronic charge, the total charge quantity collected by one electrode can be indicated by the total number of electrons on this electrode.

(iii) To decode the location of event coordinates by using the decoding formula (1).

Figure 2 shows the coordinates of the location decoded with different sizes of charge clouds and the coordinate of event used in this simulation is (20, 20). The simulation results show shat there are large deviations between the decoded coordinates and the actual coordinates when the charge cloud size is small; the coordinates decoded by the TWA become stable and close to the actual coordinates when the charge cloud sizes increase. Thus, the footprints of the charge clouds collected by TWA should not be too small, otherwise the decoding errors will be increased and the spatial resolution will be decreased.

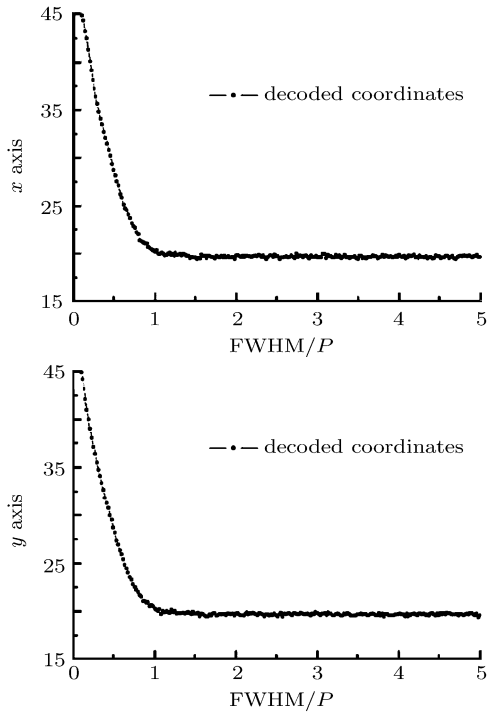


Fig. 2. Decoding results with different sizes of charge clouds, with P denoting the pitch width of anode.

To quantify the decoding error, we also use the standard deviation σ to measure the decoding errors caused by different sizes of charge clouds, its expression is

$$\sigma = \sqrt{\frac{\sum_{i=1}^{N} (x_i - x_i')^2 + (y_i - y_i')^2}{N}}, \tag{3}$$

where (x_i, y_i) and (x_i', y_i') are the original coordinates and the decoded coordinates, respectively, and figure 3 shows the simulation results. One can see that the deviation is large when the charge cloud radius is small and the error becomes stable when the charge cloud size increases. This is also consistent with previous simulation results.

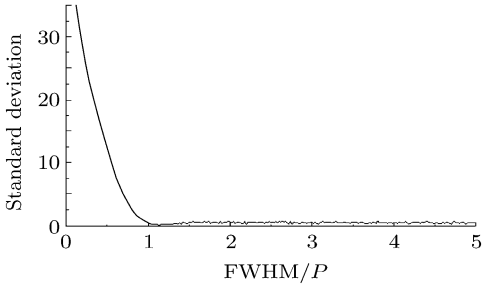
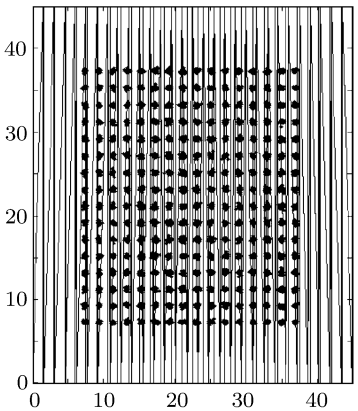


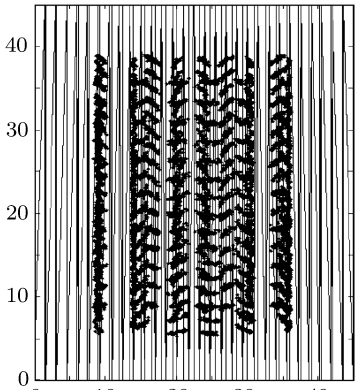
Fig. 3. Simulation results of standard deviation, with P denoting the pitch width of anode.

3.2. Simulation of imaging with different sizes of charge clouds

According to previous simulation results, we simulate the image decoded by TWA with different sizes of charge clouds. The mask used here was a pinhole matrix with 200-μm pinholes, any two of which were spaced by 2 mm. The simulation results shown in Fig. 4. Figures 4(a) and 4(b) are the decoded images with FWHM/P ratio of 3 and 1, respectively. One can see that the image shows a good linearity when FWHM/P ratio is 3, and the image shows a large decoding error when the charge cloud is small.



(a) FWHM/P = 3



(b) FWHM/P = 1

Fig. 4. Simulation results of the decoded image with different sizes of charge clouds, with P denoting the pitch width of anode.

4. Experiment

A TWA pattern with a pitch of 1.5 mm and an active area of 40-mm in diameter, using copper conductors on a 0.4-mm-thick FR4 substrate, was manufactured by laser machining equipment. The properties of the TWA were tested by using a UV photon counting imaging system based on the induction readout. In this experiment, the UV source was a mercury lamp and we did not use a photocathode. A pair of matched MCPs, with a diameter of 50 mm, was used in a chevron configuration. The channels of the MCP had a diameter of 25 μm, a length-to-diameter ratio of 40:1, and a bias angle of 6°. A Ge-layer of 200-nm thickness was deposited directly onto a 1.5-mm-thick ceramic substrate and a 253.7(±6.0)-nm filter was used to select the required wavelength. The distance between the MCP stack and the Ge-layer was 1.2 mm. Under these test conditions, previous studies have shown that the induced charges produced on the anode can reach the necessary size to ensure accurate decoding.[12,13]

4.1. Pulse-height distribution (PHD)

MCPs are the workhorse amplification step in the photon counting imaging system. Their gain, PHD and background are some of the important properties that determine detector performance. PHD is the graphical representation of the distribution of the amplitudes of output pulses for a detector at a given applied voltage. The gain-saturated mode is the MCP detector operation mode for which all output pulses have nearly the same amplitudes due to space charge saturation. In a photon-counting detector, it is necessary to operate in a gain-saturated mode so that the smaller signal pulses are amplified up to the same level as that of large saturated signal pulses while a gap still remains between the heights of signal and noise pulse. Therefore, all the signal pulses are expected to have a similar pulse height at the output. By taking advantage of the difference between signal and noise pulses, a threshold voltage can be chosen to eliminate noise pulses and a higher signal-to-noise ratio can be obtained.[17] Gain-saturated MCP Chevrons and Z-stacks produce a quasi-Gaussian[18] PHD when operated at sufficient gain. However, background PHD is essentially a negative exponent. Figure 5 shows the PHDs of the photon-counting process under different MCP voltages when the MCP-Ge layer voltage is –300 V. The curves shift toward higher pulse heights as the voltage increases. The PHDs of the MCP stack has a quasi-Gaussian shape when the MCP voltage is –1900 V (or higher), which indicates that the MCP gradually turns into the gain-saturated mode.

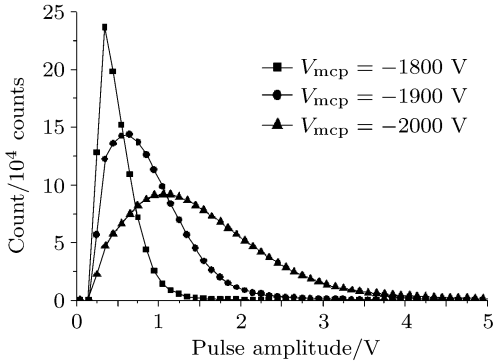


Fig. 5. Pulse height distribution curves with light incidence under different MCP voltages.

4.2. Linearity

The imaging linearity of the TWA collector is inherently good due to the correspondence of the anode geometry to the linear coordinates. A self-designed pinhole mask was used to test the linearity of the photon-counting imaging system. The pinholes had a diameter of 25 μm, with a horizontal spacing of 1300 μm and vertical spacing of 650 μm. Figure 6(a) shows the photon counting image of pinhole mask, with 20-min integration time, when the MCP voltage was –1800 V, the MCP-Ge layer voltage was −300 V and the potential of the Ge layer and the TWA was ground potential. Figure 6(b) is the normalized column density maps of the x (bottom) axis and y (upper) axis. The results show that the linearity per-

formance of the system is good. The observed maximal deviations occur on the edges of the field of view and this distortion could be due to the fact that the footprint of charge cloud goes beyond the edge of the effective collection area of the anode.

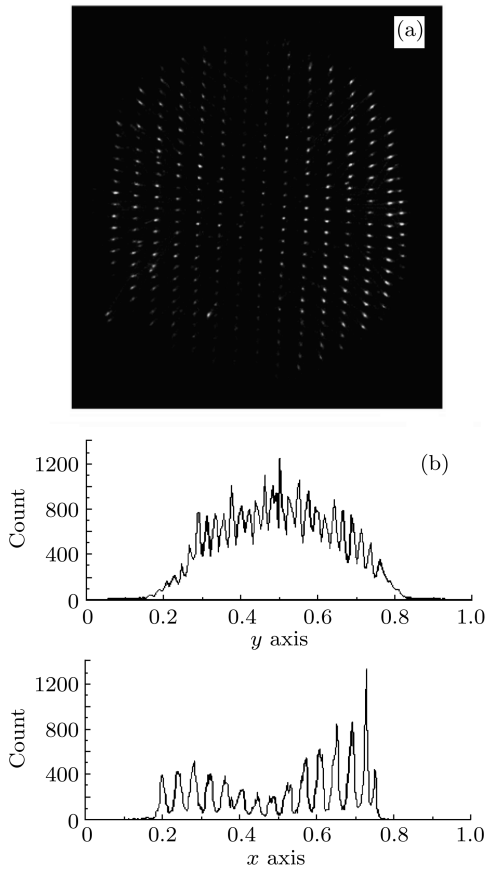


Fig. 6. Photon counting image of pinhole mask, with a horizontal spacing of 1300 μm and vertical spacing of 650 μm, using 253.7-nm illumination (a), and the normalized column density map of the x (bottom) axis and y (upper) axis (b).

4.3. Spatial resolution

A US Air Force 1951 resolution mask, which is generally used as a standard method, was used to test the spatial resolution of the system. After attenuation from one filter and 7 attenuators, the light intensity is approximately equal to 2.1×10^{-12} W/mm^2 at a wavelength of 254 nm. Figure 7 shows the resolution-mask image, with 50-min integration time, when the MCP voltage was –1850 V, the MCP-Ge layer voltage was –300 V and the potential of the Ge layer and the TWA was ground potential. The result shows that the spatial resolutions of the system along the x and the y axes are both about 99 μm (group 2 element 3 is clearly resolved).

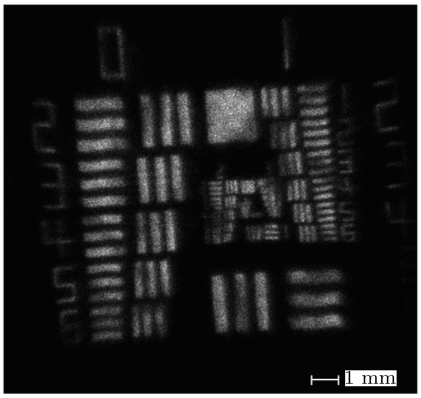


Fig. 7. Photon-counting image obtained by the USAF1951 resolution mask.

5. Conclusion

We designed a tetra wedge anode and simulated its decoding process using the Monte Carlo method. The influence of charge cloud size on the accuracy of decoding is studied. The simulation results show that the charge clouds collected by the anode should reach a certain size to ensure the accuracy of decoding. This also provides a theoretical basis for the actual design and development of TWA detector. A photon counting imaging system based on the TWA readout is set up and the linearity and spatial resolution of the system are tested. Experimental results show a good linearity and the spatial resolution is better than 100 μm. Next, the TWA will be further optimized to improve imaging performance.

References

[1] lkeda T, Kanai Y, Kojima T M, Lwai Y, Kambara T, Yamazaki Y, Hoshino M, Nebiki T and Narusawa T 2006 *Appl. Phys. Lett.* **89** 163502

[2] MacQueen H A, Mattacks C A and Roberts D R 2000 *J. Fluoresc.* **10** 301

[3] Maia J M, Mörmann D, Breskin A, Chechik R, Veloso J F C A and dos Santos J M F 2007 *Nucl. Instrum. Method* A **580** 373

[4] Andrews G B, Zurbuchen T H, Mauk B H, Malcom H, Fisk L A, Gloeckler G, Ho G C, Kelley J S, Koehn P L, LeFevere T W, Livi S S, Lundgren R A and Raines J M 2007 *Space Sci. Rev.* **131** 523

[5] Wiza J L, Henkel P R and Roy R L 1977 *Rev. Sci. Instrum.* **48** 1217

[6] Martin C, Jelinsky P, Lampton M, Malina R F and Anger H O 1981 *Rev. Sci. Instrum.* **52** 1067

[7] Lapington J S, Sanderson B, Worth L B C and Tandy J A 2002 *Nucl. Instrum. Method* A **477** 250

[8] Siegmund O H W, Vallerga J V, Martin A, Feller B, Arif M, Hussey D S and Jacobson D L 2007 *Nucl. Instrum. Method* A **579** 188

[9] Lapington J S, Howorth J R and Milnes J S 2007 *Nucl. Instrum. Method.* A **573** 243

[10] Zhang X H, Zhao B S, Zhao F F, Liu Y A, Zhu X P and Yan Q R 2009 *Nucl. Instrum. Method* A **610** 724

[11] Zhang X H, Zhao B S, Zhao F F, Liu Y A, Miao Z H, Zhu X P and Yan Q R 2009 *Rev. Sci. Instrum.* **80** 033101

[12] Zhao F F, Zhao B S, Liu Y A, Hu H J and Cao X B 2010 *Acta Phys. Sin.* **59** 6306 (in Chinese)

[13] Zhao F F, Liu Y A, Hu H J and Zhao B S 2010 *Acta Phys. Sin.* **59** 7096 (in Chinese)

[14] Lapington J S, Howorth J R and Milnes J S 2005 *Proc. SPIE* **5881** 588109

[15] Saito M, Saito Y, Asamura K and Mukai T 2007 *Rev. Sci. Instrum.* **78** 023302

[16] Smith A, Kessel R, Lapington J S and Walton D M 1989 *Rev. Sci. Instrum.* **60** 3509

[17] Qu D N and Dainty J C 1988 *Adv. Electr. Electron. Phys.* (New York: Academic) **74** 107

[18] Bush B C, Cotton D M, Siegmund O H W, Chakrabarti S, Harris W M and Clarke J T 1991 *Proc. SPIE* **1549** 290